Plant Physiology, March 2000, Vol. 122, pp. 775–781, www.plantphysiol.org © 2000 American Society of Plant Physiologists

Spatial Regulation of Pectic Polysaccharides in Relation to Pit Fields in Cell Walls of Tomato Fruit Pericarp[1]

Caroline Orfila and J. Paul Knox*

Centre for Plant Sciences, University of Leeds, Leeds LS2 9JT, United Kingdom

Scanning electron microscopic examination of intact tomato (*Lycopersicon esculentum*) pericarp and isolated pericarp cell walls revealed pit fields and associated radiating ridges on the inner face of cell walls. In regions of the cell wall away from pit fields, equivalent ridges occurred in parallel arrays. Treatment of isolated cell walls with a calcium chelator resulted in the loss of these ridges, indicating that they contain homogalacturonan-rich pectic polysaccharides. Immunolabeling procedures confirmed that pit fields and associated radiating ridges contained homogalacturonan. Epitopes of the side chains of pectic polysaccharides were not located in the same regions as homogalacturonan and were spatially regulated in relation to pit fields. A (1→4)-β-galactan epitope was absent from cell walls in regions of pit fields. A (1→5)-α-arabinan epitope occurred most abundantly at the inner face of cell walls in regions surrounding the pit fields.

The retention of a fibrous composite cell wall at the cell surface has many consequences for cell functioning and, in particular, has impact on the nature of the interactions that occur between plant cells. It is now recognized that the symplastic links formed by plasmodesmata across cell walls are important channels not only for the movement of low-M_r compounds, but also for the specific trafficking of macromolecules, including proteins and nucleic acids (Mezitt and Lucas, 1996; Ghoshroy et al., 1997; Kragler et al., 1998a). Macromolecular signals trafficked within interconnected areas of tissues or organs, known as symplastic domains, are likely to underpin important aspects of cell and plant development (Cooke et al., 1996; McLean et al., 1997; Kragler et al., 1998a).

There is some information available on the structure of primary and secondary plasmodesmata (Robards and Lucas, 1990; Ding et al., 1992). The formation of primary plasmodesmata has been observed by electron microscopy, and mechanisms concerning the positioning of the ER and the fusion of vesicles at the cell plate to form the middle lamella around the plasmodesmal pore have been suggested (Hepler, 1982). Little is known of the mechanisms leading to local cell wall breakdown that occur during the insertion of secondary plasmodesmata, although it generally occurs in thin regions of the cell wall (Ding and Lucas, 1996). The formation of secondary plasmodesmata can be induced in graft unions (Kollmann and Glockmann, 1991) and in regenerating cultures (Monzer, 1991) and probably involves the action of hemicellulases and pectinases (Ding and Lucas, 1996). Plasmodesmata are often grouped together in areas of cell walls known as pit fields. Aspects or changes in cell wall architecture that accommodate primary plasmodesmata formation, the insertion of secondary plasmodesmata, and pit field formation are not well documented. There are some reports of specialized cell wall structures that appear to form a collar around plasmodesmata (Badelt et al., 1994; Turner et al., 1994), although the precise nature and function of these structures are not clear.

The pectic polysaccharides are major components of the primary cell wall matrix. There are three major classes of pectic polysaccharides in higher plants: homogalacturonan (HG), rhamnogalacturonan I (RGI), and rhamnogalacturonan II (RGII) (Albersheim et al., 1996). Together these form a complex group of polysaccharides with considerable potential for structural modulation leading to alteration of cell wall properties such as adhesion between cells, porosity, and stiffness. Some preliminary data on the occurrence of pectic polysaccharides in relation to pit fields have been reported. Roy et al. (1997) described microdomains of HG epitopes and acidic sites in the cell wall in the region of pit fields of apple fruit cortex cells. Casero and Knox (1995) reported the abundance of HG at pit fields and HG-rich structures radiating out from pit fields on the inner face of cell walls of tomato (*Lycopersicon esculentum*) pericarp cells.

In this report we extend the observations made by Casero and Knox (1995) and describe the occurrence of ridges at the inner face of tomato pericarp cell walls as revealed by scanning electron microscopy (SEM). Furthermore, using highly defined antibody probes to epitopes known to occur in HG and the side chains of RGI, we report the spatial regulation of these epitopes in relation to pit fields.

MATERIALS AND METHODS

Plant Material

Tomato (*Lycopersicon esculentum* cv Ailsa Craig) plants were grown under standard greenhouse conditions and fruit were harvested at the mature green stage (35 d post anthesis). Tomato fruit were kindly provided by Dr. G.B. Seymour (Horticulture Research International, Warwick, UK).

[1] C.O. was supported by a U.K. Biotechnology and Biological Science Research Council CASE studentship with Horticulture Research International.

* Corresponding author; e-mail j.p.knox@leeds.ac.uk; fax 44–113–2333144.

Monoclonal Antibodies and Immunochemistry on Nitrocellulose

The anti-pectin monoclonal antibodies used have all been described previously. JIM5 (anti-HG; Knox et al., 1990), LM5 (anti-[1→4]-β-D-galactan; Jones et al., 1997), and LM6 (anti-[1→5]-α-L-arabinan; Willats et al., 1998) were used unpurified from hybridoma supernatants. The anti-callose (1→3)-β-D-glucan antibody (Meikle et al., 1991) was obtained from Biosupplies (Parkville, Victoria, Australia).

To confirm that LM5 and LM6 did not bind to glycoproteins or proteoglycans occurring in tomato pericarp cells, mature green pericarp material was homogenized in SDS-PAGE sample buffer and analyzed by western blotting and immunodot assays using procedures described elsewhere (Smallwood et al., 1996). LM1 (anti-Hyp-rich glycoprotein; Smallwood et al., 1995) and LM2 (anti-arabinogalactan-protein; Smallwood et al., 1996) were used as control antibodies for the probing of pericarp homogenates.

SEM

Tomato fruit were washed and the pericarp was cut into large cubes (1 cm^3). The cubes were frozen under liquid nitrogen and fractured using a pestle so that small fragments (approximately 0.03 cm^3) were obtained. The pericarp fragments were fixed in 2.5% (w/v) glutaraldehyde in 0.1 M sodium phosphate buffer, pH 7.2, for 2 h at 4°C, washed extensively with sodium phosphate buffer, and subsequently post-fixed in 1% (w/v) osmium tetroxide in sodium phosphate buffer for 1 h at 4°C. The fragments were washed extensively with sodium phosphate buffer and dehydrated in an acetone series (10%–100%). Dehydrated fragments were critical-point dried, mounted onto metal studs, coated with colloidal gold, and viewed using a scanning electron microscope (CamScan, Leica, Cambridge, UK). For observation of isolated cell wall preparations, cell wall material was prepared as described below and then dispersed onto adhesive tape, which was then mounted onto metal studs, coated with colloidal gold, and examined as above.

Preparation of Enzyme-Free Cell Wall Material

Cell wall material was prepared as described in Seymour et al. (1990). Fruit were washed, peeled, and the pericarp cut into small cubes (0.125 cm^3), which were then homogenized in 4 volumes of acetone at −20°C using a polytron homogenizer. The homogenate was filtered through Miracloth (Calbiochem-Novabiochem, San Diego) and washed with 80% and 100% acetone (12.5 mL g^{-1} tissue fresh weight). Acetone-insoluble solids were suspended in a solution of PAW (phenol:acetic acid:water, 2:1:1, w/v, 10 mL g^{-1} tissue fresh weight) and the mixture stirred for 15 min at 4°C. After PAW treatment, acetone was added to a final concentration of 80% and the mixture filtered though a sintered glass filter. The filtrate was washed with 100% acetone (200 mL) to remove traces of PAW. The obtained cell wall material was dried over P_2O_5 under vacuum and stored desiccated at −20°C until needed. Calcium-bound pectin was extracted from the cell wall material by incubation in a solution containing 0.1 M CDTA (trans-1,2-

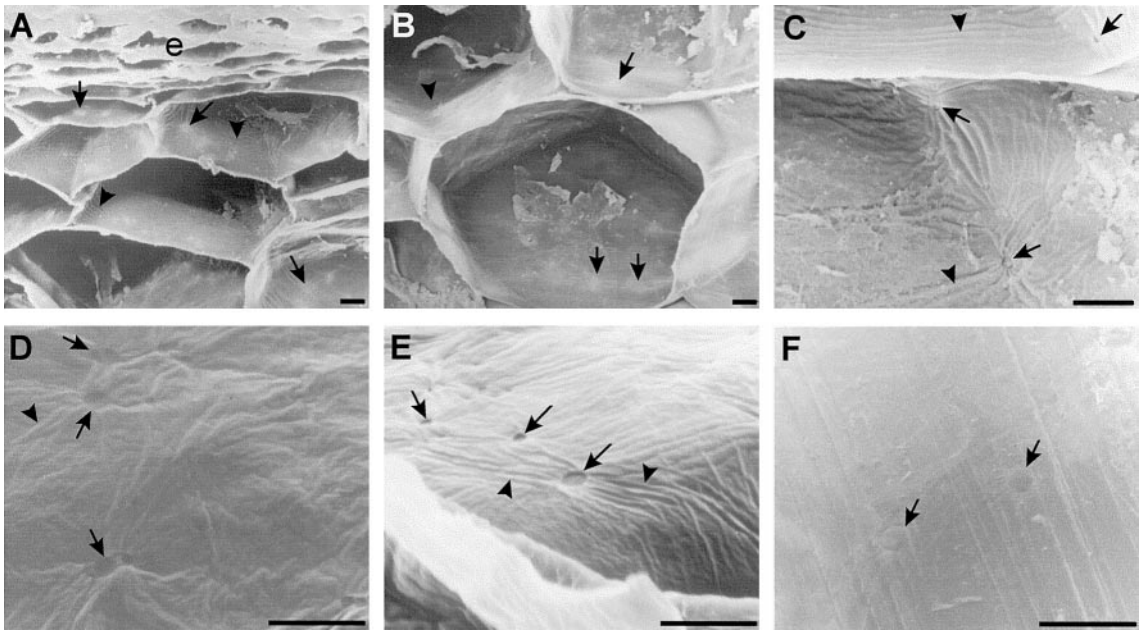

Figure 1. Scanning electron micrographs of the inner face and pit fields of mature green tomato pericarp cell walls. A to C, Freeze-fracture surfaces of intact pericarp, exposing the inner surface of cell walls and showing pit fields (arrows) and associated ridges (arrowheads). A shows exocarp (e) and B and C inner mesocarp cells. D and E, Isolated cell wall material retains pit field and ridge structures. F, After extraction of pectin from isolated cell walls with CDTA, pit fields can still be identified, but the ridges are not apparent. All scale bars = 10 μm.

diaminocyclo-hexane-*N,N,N′,N′*-tetra-acetic acid) (Sigma-Aldrich, St. Louis), pH 6.5, for 6 h, then washed with distilled water, followed by a second incubation in 0.1 M CDTA for 2 h and washing with distilled water. All incubations were done at room temperature with gentle rocking. The cell wall material was then dehydrated in an acetone series and dried over P_2O_5 under vacuum.

Preparation of Material for Microscopy

Pericarp cubes (0.06 cm^3) were fixed in 2.5% (w/v) glutaraldehyde in 0.1 M sodium phosphate buffer, pH 7.2, for 2 h at 4°C, then washed extensively with sodium phosphate buffer. The cubes were dehydrated in an ethanol series (70%–100%), then infiltrated with LR White resin (London Resin, Reading, UK). The cubes were then placed in gelatin capsules containing LR White resin and allowed to polymerize at 37°C for 5 d.

Immunofluorescence Labeling for Light Microscopy

Sections obtained from the resin-embedded material (0.5 μm thickness) were incubated in a 5% (w/v) solution of fat-free milk powder in phosphate buffered saline (PBS), pH 7.2, for 30 min. Sections were then incubated for 1 h in a solution containing anti-HG JIM5, anti-(1→4)-β-galactan LM5, or anti-(1→5)-α-arabinan LM6 (rat monoclonal antibodies) diluted 1:10 in milk powder/PBS or anti-(1→3)-β-glucan (mouse monoclonal antibody) diluted 1:100 in milk powder/PBS. The sections were then washed extensively with milk powder/PBS and subsequently incubated for 1 h in a solution containing goat anti-rat IgG (for JIM5, LM5, and LM6) or sheep anti-mouse IgG [for anti-(1→3)-β-glucan] linked to FITC (fluorescein isothiocyanate) (Sigma) diluted 1:100 in milk powder/PBS. Sections were washed extensively with PBS, then mounted in a PBS/fluorescence anti-fade solution (Citifluor AF3, Agar Scientific, Stansted, Essex, UK) and viewed with a microscope equipped with epifluorescence illumination. All incubations were done at room temperature. For cytochemical staining of callose, sections were incubated for 2 min at room temperature in a solution of 0.05% (w/v) aniline blue in 0.1 M Gly, pH 9.5. The sections were washed extensively with PBS and mounted as previously described. For immunofluorescence labeling, cell wall preparations were suspended in distilled water and allowed to rehydrate. The preparations were then labeled by suspension in the antibody solutions prepared as described for the labeling of sections. The preparations were washed by re-suspension, mounted, and examined.

Immunogold Labeling for Electron Microscopy

Sections obtained from the resin-embedded material (0.1 μm thickness) were incubated in 3% (w/v) bovine serum albumin (BSA) (Sigma) in PBS for 30 min. Sections were then incubated for 1 h in a solution containing anti-HG JIM5, anti-(1→4)-β-galactan LM5, or anti-(1→5)-α-arabinan LM6 monoclonal antibodies, diluted 1:10 in BSA/PBS. The sections were washed five times in BSA/PBS, and then incubated in a solution containing goat anti-rat IgG coupled to 10 nm colloidal gold (Sigma) diluted 1:50 in BSA/PBS. The sections were washed extensively with PBS and then with distilled water, stained with 4% (w/v) uranyl acetate for 15 min, then washed extensively with distilled water. All incubations were at room temperature. Sections were examined with an electron microscope (model 1200 ex, JEOL, Tokyo).

RESULTS

Aspects of Cell Wall Architecture at the Inner Face of Tomato Pericarp Cell Walls Revealed by SEM

Examination by SEM of a radially cut face of mature green tomato pericarp revealed that protoplasts had been readily lost during specimen preparation, allowing the inner face of the cell walls that had been adjacent to the plasma membrane to be observed, as shown in Figure 1, A to C. Several structural features of these cell walls were observed, including circular depressions corresponding to

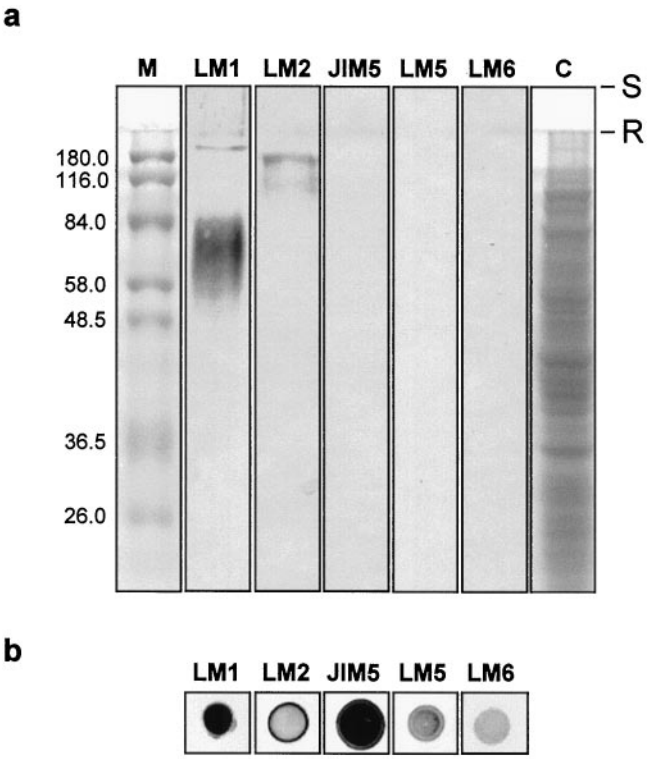

Figure 2. Western blotting and immunodot assay of mature green tomato pericarp. a, Supernatant from a homogenate of mature green tomato pericarp was separated by SDS-PAGE (13 μg of protein in each lane), transferred to nitrocellulose, and probed with the monoclonal antibodies LM1 (anti-Hyp-rich glycoprotein), LM2 (anti-arabinogalactan-protein), JIM5 (anti-HG), LM5 [anti-(1→4)-β-galactan], and LM6 [anti-(1→5)-α-arabinan]. Lane C, Total protein stained with Coomassie blue; lane M, molecular mass markers (in kD); S and R indicate top of stacking and resolving gels, respectively. b, Immunodot assay of 1-μL (0.65 μg of protein) aliquots of supernatant samples used in a probe with the same series of monoclonal antibodies.

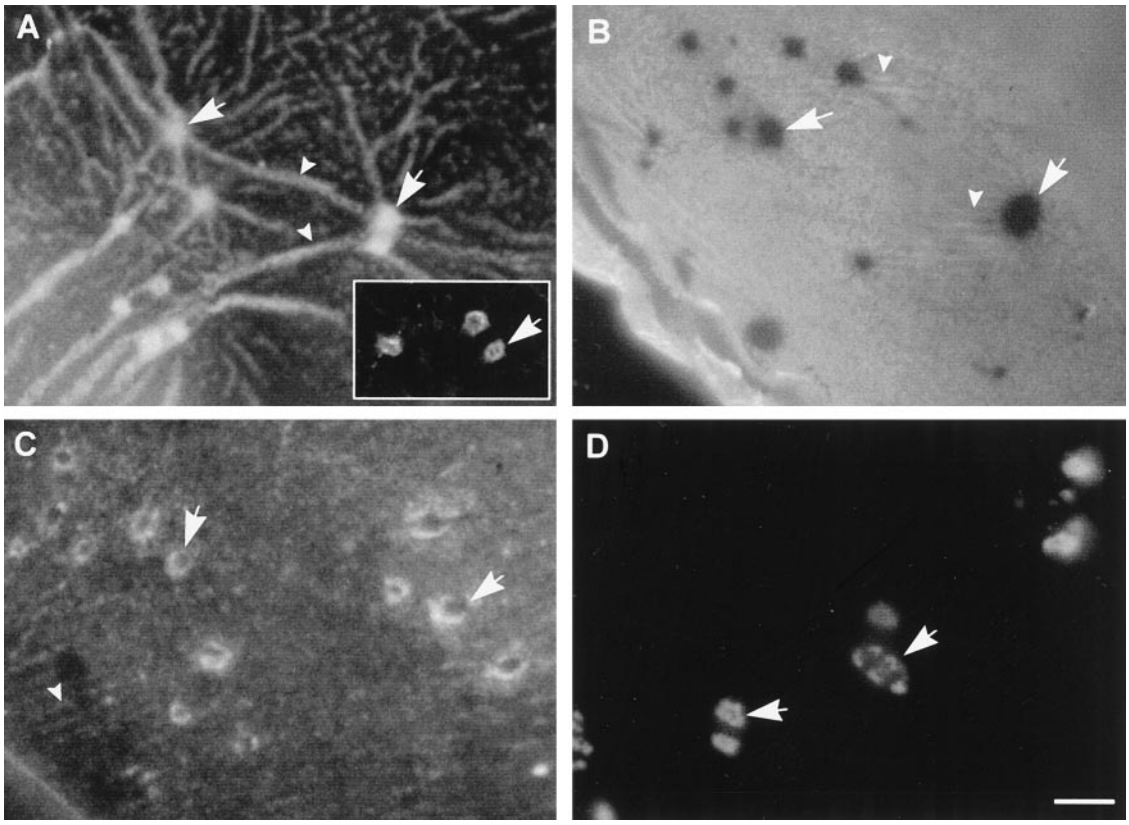

Figure 3. Immunofluorescent labeling of polysaccharide epitopes at the inner face of isolated cell walls of mature green tomato pericarp. A, The JIM5 HG epitope is abundant at pit fields (arrows) and radiating ridges (arrowheads). In CDTA-extracted walls, the JIM5 epitope is still located at pit fields but not on the surrounding cell wall surface (inset). B, The LM5 (1→4)-β-galactan epitope is abundant at the cell wall surface but absent from the regions of pit fields. There is some indication that the LM5 epitope occurs in structures radiating out from the pit field regions (arrowheads). C, The LM6 (1→5)-α-arabinan epitope is most abundant on the cell wall surface at the edge of pit fields. There is some indication of the occurrence of the LM6 epitope in ridges in other regions of the cell wall face (arrowhead). D, A callose [(1→3)-β-glucan] epitope is closely associated with pit fields and does not occur in any other region of the cell wall surface. Scale bar = 5 μm.

pit fields and ridge-like features radiating out from the pit fields, with widths in the region of 80 to 140 nm and spaced by 300 to 350 nm. These are likely to correspond to the HG-rich pectic structures previously reported at the inner face of ripe tomato pericarp cells (Casero and Knox, 1995). Other than that they contain HG epitopes, nothing previously has been reported concerning the structure or function of these ridges, and, to our knowledge, they have not previously been investigated by SEM. In the scanning electron micrographs of intact pericarp cells, it can be seen that in regions of the cell wall not in the vicinity of pit fields, the ridges often occur in parallel series, as shown in Figure 1, A to C.

To examine these ridges in more detail, cell walls were isolated from mature green tomato pericarp by acetone extraction. Examination of isolated cell walls by SEM indicated that surface features were retained, as shown in Figure 1, D and E. Treatment of isolated cell walls with a calcium chelator (CDTA) resulted in the loss of the ridges and the appearance of a much smoother cell wall surface when examined by SEM, as seen in Figure 1F, providing evidence that HG is a major component of these structures.

Pectic Epitopes Are Spatially Organized in Relation to Pit Fields and Inner Cell Wall Ridges

The ridges of pectic material at the cell wall surface and cell wall domains around pit fields were examined further with a range of anti-pectin monoclonal antibodies, including anti-(1→4)-β-galactan and anti-(1→5)-α-arabinan monoclonal antibodies that have been generated using synthetic neoglycoproteins (Jones et al., 1997; Willats et al., 1998). (1→4)-β-Galactan and (1→5)-α-arabinan are known to be components of RGI side chains (Albersheim et al., 1996). It has previously been reported that an arabinosylated (1→6)-β-galactan epitope of RGI is also carried by glycoproteins (Puhlmann et al., 1994; Steffan et al., 1995). The anti-(1→4)-β-galactan and anti-(1→5)-α-arabinan probes used here did not bind to any material on western blots of homogenized pericarp, although binding occurred in immunodot assays of the same material, as shown in Figure 2. This demonstrates that the (1→4)-β-galactan and (1→5)-α-arabinan epitopes are not carried by glycoproteins or proteoglycans, although they may occur on other, uncharacterized cell wall polysaccharides in addition to RGI.

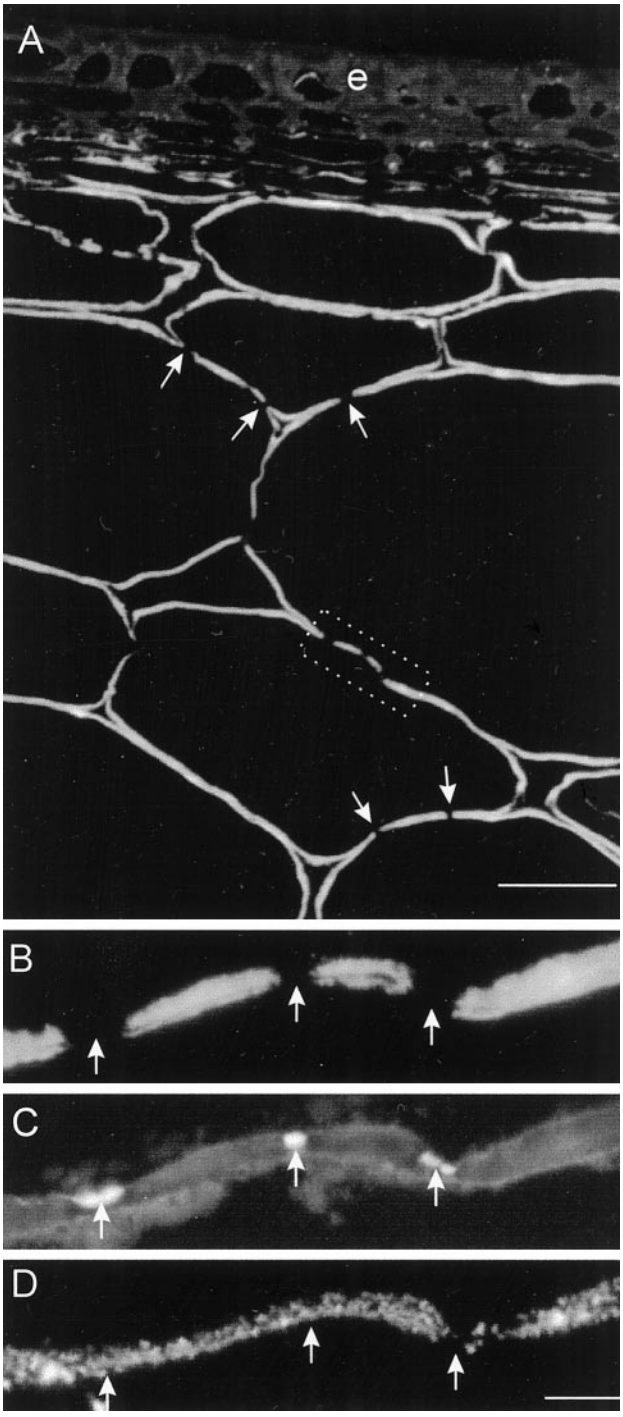

Figure 4. Immunofluorescent labeling of polysaccharide epitopes on radial sections of resin-embedded mature green tomato pericarp. A, The LM5 (1→4)-β-galactan epitope is abundant in the cell walls of pericarp parenchyma cells except for small regions 2 to 10 μm in length along the wall, where the epitope is entirely absent (arrows). e, Epidermis. Scale bar = 100 μm. Micrographs of a region of A (dashed box) dual-labeled with LM5 (B) and aniline blue (C) indicate that callose occurs in regions where the LM5 epitope is absent. D, In an adjacent serial section, the JIM5 HG epitope is present throughout the cell wall, including the regions of pit fields. Scale bar = 10 μm.

Specific patterns of the different pectic epitopes were seen when immunolabeling of the inner face was carried out on both thick sections of fresh mature green pericarp tissue and also isolated cell walls. Figure 3 shows the distribution of HG, (1→4)-β-galactan, and (1→5)-α-arabinan epitopes at the surface of isolated cell walls corresponding to the inner face of cell walls in intact pericarp. The JIM5 HG epitope occurred abundantly at pit fields and the ridges radiating out from the pit fields and in ridges in regions away from the pit fields (Fig. 3A). When the cell walls were extracted with the calcium chelator CDTA, JIM5 labeling was restricted to the pit fields and did not label the area surrounding them (Fig. 3A, inset); in contrast, (1→4)-β-galactan was absent from the cell walls in regions of the pit fields, as shown in Figure 3B. In some regions close to the pit fields, the (1→4)-β-galactan epitope was weakly associated with ridges that appeared to be thinner and more closely spaced than those identified by SEM and by JIM5. The (1→5)-α-arabinan epitope occurred most abundantly on the inner face of cell walls in regions surrounding pit fields and appeared as rings of immunofluorescence as shown in Figure 3C. The (1→5)-α-arabinan epitope did not occur in the HG-rich radiating ridges, although it occurred at a low level in parallel lines in some regions of the cell wall face (Fig. 3C). Callose labeling was restricted to pit fields, as shown in Figure 3D. Extraction of cell wall preparations with CDTA did not affect the labeling patterns with LM5, LM6, or the anti-callose antibodies (data not shown).

To study the occurrence of pectic epitopes within cell wall layers, we immunolabeled resin-embedded sections of mature green tomato pericarp cells. Immunofluorescent labeling of a radial section indicated that (1→4)-β-galactan was often absent from distinct regions of cell walls that were in the region of 2 to 10 μm in length, as shown in Figure 4A. That these regions corresponded to pit fields was indicated by the presence of callose in double-labeling experiments with aniline blue, as shown in Figure 4, B and C. Immunolabeling of a serially associated section with JIM5 did not reveal equivalent extensive gaps in the presence of the HG epitope in the cell wall, as shown in Figure 4D. These observations were confirmed by immunogold labeling of resin-embedded mature green tomato pericarp, as shown in Figure 5. (1→4)-β-Galactan was not present in cell walls in the region of pit fields or the immediate area of the cell wall surrounding it (Fig. 5A), but did occur in the primary cell wall farther away from the pit field (Fig. 5D). The absence of (1→4)-β-galactan appeared to correlate with the thinner regions of the cell wall that occur at pit fields. In contrast, the HG JIM5 epitope was present abundantly in cell walls in the region of pit fields, except at electron-translucent areas, which are likely to be callose deposits. The JIM5 HG epitope was also abundant in the primary cell wall and middle lamella in regions away from pit fields (Fig. 5E). The (1→5)-α-arabinan epitope occurred only weakly in cell walls at the mature green stage. However, judging from the low number of gold particles, the epitope was equally present in cell walls in the pit field region (Fig. 5C) and in regions distant from pit fields (Fig. 5F).

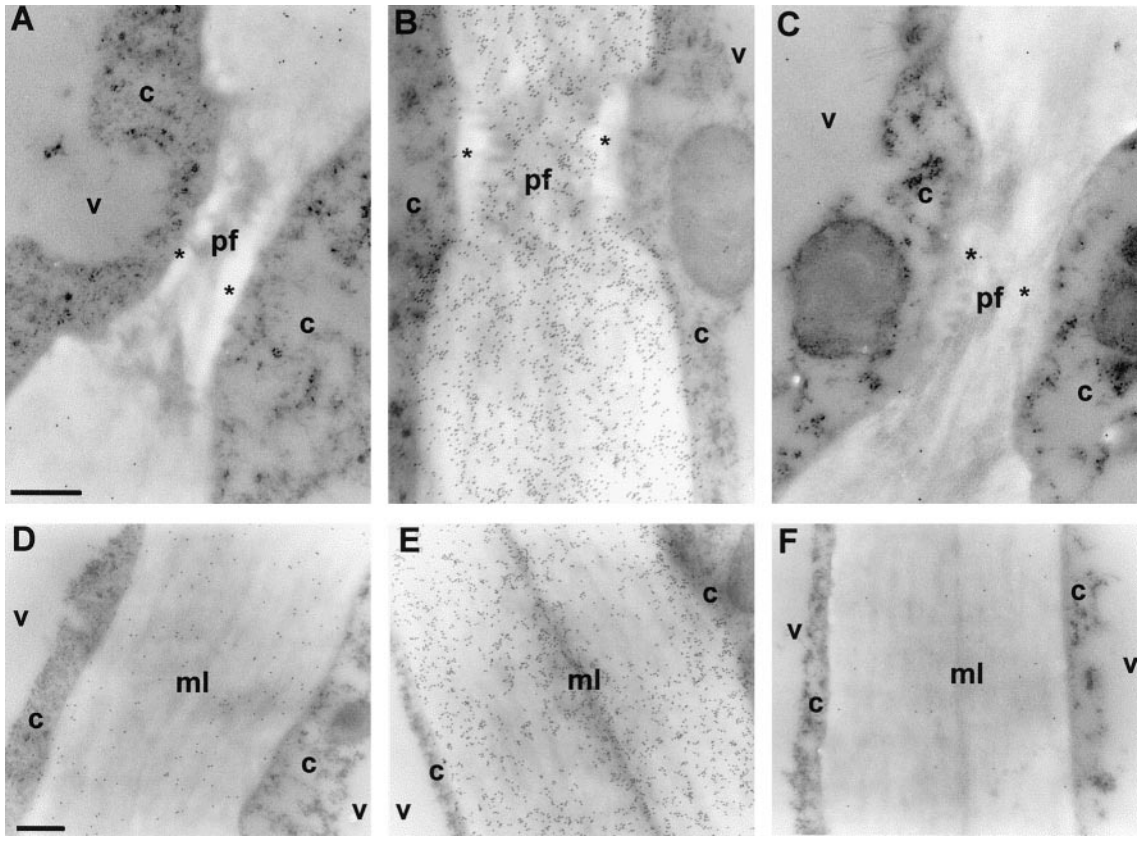

Figure 5. Immunogold electron micrographs of resin-embedded mature green tomato pericarp showing polysaccharide epitopes in cell walls at primary pit fields and surrounding regions. A, The LM5 (1→4)-β-galactan epitope is absent from the cell wall at the pit field but is present throughout the rest of the primary cell wall (D). B, The JIM5 HG epitope is abundant throughout the pit field except at electron-translucent areas (*), which are likely to be callose deposits at the plasma membrane sides of the pit field. The HG epitope is also abundant throughout the primary cell wall (E). C, The LM6 (1→5)-α-arabinan epitope is not abundant in resin-embedded material but is detected at low levels in the cell wall at both pit fields (C) and the rest of the primary cell wall (F). Scale bars = 500 nm. c, Cytoplasm; v, vacuole; pf, pit field; ml, middle lamella.

DISCUSSION

The ridges on the inner face of tomato pericarp cell walls, identified in this study by SEM, appear to contain HG. The appearance of the ridges may have been exaggerated by the drying procedure used to prepare the pericarp material for SEM, but are unlikely to be artifacts of this procedure because they reflected the labeling patterns with an anti-HG antibody of isolated cell walls in the present study (Fig. 3) and in a previous report using fresh pericarp (Casero and Knox, 1995). These combined observations indicate that HG-containing components are deposited in an oriented manner on the inner face of the pericarp cell walls. The significance of these patterns of deposition is far from clear; they may contribute to an aspect of the mechanical properties of the cells or may in some way be indicative of mechanisms of the deposition of cell wall material.

It is of considerable interest that HG, (1→4)-β-galactan, and (1→5)-α-arabinan epitopes occur in different patterns on the inner face of and within pericarp cell walls. These observations indicate that HG is separate from both (1→4)-β-galactan and (1→5)-α-arabinan at this location, and also that at least two populations of HG occur. The HG in the ridges was readily extracted with CDTA, but the HG at pit fields was not, suggesting that it was attached to the cell wall by a mechanism other than calcium cross-linking. The (1→4)-β-galactan and (1→5)-α-arabinan epitopes also have different locations, suggesting the spatial regulation of RGI side chains. The absence of (1→4)-β-galactan from cell walls throughout the region of pit fields indicates the existence of a distinct cell wall architecture in these regions. These observations were made on mature green pericarp and therefore do not reflect ripening-related phenomena. Whether the absence of this epitope reflects reduced levels of RGI or the presence of a distinct RGI is not known.

The absence of (1→4)-β-galactan is likely to result in distinctive cell wall properties, as several properties could be influenced by the presence or absence of a (1→4)-β-galactan-rich polysaccharide. The porosity of the cell wall matrix may be altered in these regions, which could determine the capacity of enzymes to reach sites of action in the pit fields. Altered mechanical properties could produce a more or less rigid cell wall matrix around plasmodesmata for the maintenance of pore integrity or for protection against mechanical stresses. The absence of (1→4)-β-

galactan from subepidermal pericarp layers and petiole collenchyma thickenings in tomato has been suggested to relate to the possible increased mechanical strength of these regions (Jones et al., 1997). The presence of (1→4)-β-galactans in the matrix of flax fibers has been proposed to contribute to tensile strength (Girault et al., 1997). Another possibility is that the cell wall matrix may be involved in the control of cell wall thickness, which is often reduced at pit fields.

The functional requirements of the cell wall regions around plasmodesmata are not clear. A combination of microchannel dilation and protein unfolding is required for the cell-to-cell trafficking of proteins, and it has been suggested that the properties of the cell wall surrounding plasmodesmata may restrict the degree to which microchannels can dilate (Kragler et al., 1998b). There are some indications that levels of cellulose are reduced in the regions of pit fields (Olesen and Robards, 1990; data not shown). It is also necessary to maintain the integrity of plasmodesmata and pit fields within expanding cell walls, and we observed cell wall domains without (1→4)-β-galactan of equivalent size and frequency in 10-d-old fruit. However, we were unable to detect (1→4)-β-galactan in cell plates in early-stage pericarp (data not shown). At the mature green stage, the (1→5)-α-arabinan epitope is associated with a highly soluble polysaccharide and was present in cell walls of sections and preparations at only a low level. The (1→5)-α-arabinan epitope did not occur in sections of 10-d-old fruit, but appeared abundantly in cell walls of sections in which pit fields had already fully formed (data not shown). The pattern of the occurrence of the (1→5)-α-arabinan epitope reported here may relate to the position and maintenance of pit fields in expanding cell walls or to the direction of deposition of other cell wall components.

The results of the present study extend our appreciation of the complexity of pectic polysaccharides and of the spatial regulation of cell wall components, and also provide a basis for further studies on the cell wall in relation to pit field formation and maintenance.

Received August 2, 1999; accepted November 8, 1999.

LITERATURE CITED

Albersheim P, Darvill AG, O'Neill MA, Schols HA, Voragen AGJ (1996) An hypothesis: the same six polysaccharides are components of the primary cell walls of all higher plants. *In* J Visser, AGJ Voragen, eds, Pectins and Pectinases. Elsevier Science BV, Amsterdam, pp 47–55

Badelt K, White RG, Overall RL, Vesk M (1994) Ultrastructural specializations of the cell wall sleeve around plasmodesmata. Am J Bot **81:** 1422–1427

Casero PJ, Knox JP (1995) The monoclonal antibody JIM5 indicates patterns of pectin deposition in relation to pit fields at the plasma-membrane-face of tomato pericarp cell walls. Protoplasma **188:** 133–137

Cooke TJ, Tilney MS, Tilney LG (1996) Plasmodesmal networks in apical meristem and mature structures: geometric evidence of both primary and secondary formation of plasmodesmata. *In* M Smallwood, JP Knox, DJ Bowles, eds, Membranes: Specialized Functions in Plants. BIOS Scientific Publishers, Oxford, pp 471–486

Ding B, Lucas WJ (1996) Secondary plasmodesmata: biogenesis, special functions and evolution. *In* M Smallwood, JP Knox, DJ Bowles, eds, Membranes: Specialized Functions in Plants. BIOS Scientific Publishers, Oxford, pp 489–503

Ding B, Turgeon R, Parthasarathy MV (1992) Substructure of freeze-substituted plasmodesmata. Protoplasma **169:** 28–41

Ghoshroy S, Lartey R, Sheng JS, Citovsky V (1997) Transport of proteins and nucleic acids through plasmodesmata. Annu Rev Plant Physiol Plant Mol Biol **48:** 25–48

Girault R, Bert F, Rihouey C, Jauneau A, Morvan C, Jarvis M (1997) Galactans and cellulose in flax fibres: putative contributions to the tensile strength. Int J Biol Macromol **21:** 179–188

Hepler PK (1982) Endoplasmic reticulum in the formation of the cell plate and plasmodesmata. Protoplasma **111:** 121–133

Jones L, Seymour GB, Knox JP (1997) Localization of pectic galactan in tomato cell walls using a monoclonal antibody specific to (1→4)-β-D-galactan. Plant Physiol **113:** 1405–1412

Knox JP, Linstead PJ, King J, Cooper C, Roberts K (1990) Pectin esterification is spatially regulated both within cell walls and between developing tissues of root apices. Planta **181:** 512–521

Kollmann R, Glockmann C (1991) Studies on graft unions. III. On the mechanism of secondary formation of plasmodesmata at the graft interface. Protoplasma **165:** 71–85

Kragler F, Lucas WJ, Monzer J (1998a) Plasmodesmata: dynamics, domains and patterning. Ann Bot **81:** 1–10

Kragler F, Monzer J, Shash K, Xoconostle-Cázares B, Lucas WJ (1998b) Cell-to-cell transport of proteins: requirement for unfolding and characterization of binding to a putative plasmodesmal receptor. Plant J **15:** 367–381

McLean BG, Hempel FD, Zambryski P (1997) Plant intercellular communication via plasmodesmata. Plant Cell **9:** 1043–1054

Meikle PJ, Bonig I, Hoogenraad NJ, Clarke AE, Stone BA (1991) The location of (1–3)-β-glucans in the walls of pollen tubes of *Nicotiana alata* using a (1–3)-β-glucan-specific monoclonal antibody. Planta **185:** 1–8

Mezitt LA, Lucas WJ (1996) Plasmodesmal cell to cell transport of proteins and nucleic acids. Plant Mol Biol **23:** 251–273

Monzer J (1991) Ultrastructure of secondary plasmodesmata formation in regenerating *Solanum nigrum*-protoplast cultures. Protoplasma **165:** 86–95

Olesen P, Robards AW (1990) The neck region of plasmodesmata: general architecture and some functional aspects. NATO ASI Ser Ser H **46:** 145–170

Puhlmann J, Bucheli E, Swain MJ, Dunning N, Albersheim P, Darvill AG, Hahn MG (1994) Generation of monoclonal antibodies against plant cell wall polysaccharides. I. Characterization of a monoclonal antibody to a terminal α-(1→2)-linked fucosyl-containing epitope. Plant Physiol **104:** 699–710

Robards AW, Lucas WJ (1990) Plasmodesmata. Annu Rev Plant Physiol Plant Mol Biol **41:** 369–419

Roy S, Watada AE, Wergin WP (1997) Characterization of the cell wall microdomain surrounding plasmodesmata in apple fruit. Plant Physiol **114:** 539–547

Seymour GB, Colquhoun IJ, DuPont MS, Parsley KR, Selvendran RR (1990) Composition and structural features of cell wall polysaccharides from tomato fruits. Phytochemistry **29:** 725–731

Smallwood M, Martin H, Knox JP (1995) An epitope of rice threonine- and hydroxyproline-rich glycoprotein is common to cell wall and hydrophobic plasma membrane glycoproteins. Planta **196:** 510–522

Smallwood M, Yates EA, Willats WGT, Martin H, Knox JP (1996) Immunochemical comparison of membrane-associated and secreted arabinogalactan-proteins in rice and carrot. Planta **198:** 452–459

Steffan W, Kovác P, Albersheim P, Darvill AG, Hahn MG (1995) Characterization of a monoclonal antibody that recognizes an arabinosylated (1→6)-β-D-galactan epitope in plant complex carbohydrates. Carbohydr Res **275:** 295–307

Turner A, Wells B, Roberts K (1994) Plasmodesmata of maize root tips: structure and composition. J Cell Sci **107:** 3351–3361

Willats WGT, Marcus SE, Knox JP (1998) Generation of a monoclonal antibody specific to (1→5)-α-L-arabinan. Carbohydr Res **308:** 149–152